



# Direct sludge granulation by applying mycelial pellets in continuous-flow aerobic membrane bioreactor: Performance, granulation process and mechanism

Xiao Xiao<sup>a</sup>, Fang Ma<sup>a</sup>, Shijie You<sup>a</sup>, Haijuan Guo<sup>b,c,\*</sup>, Jinna Zhang<sup>a</sup>, Xiaotong Bao<sup>c</sup>, Xiping Ma<sup>b</sup>

<sup>a</sup> State Key Laboratory of Urban Water Resource and Environment, School of Environment, Harbin Institute of Technology, Harbin 150090, PR China

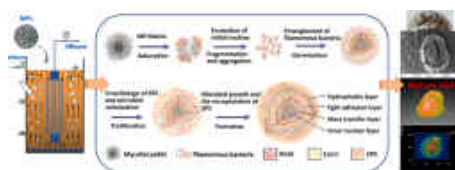
<sup>b</sup> School of Environment, Liaoning University, Shenyang 110036, PR China

<sup>c</sup> College of Energy and Environmental Engineering, Hebei University of Engineering, Handan 056038, PR China

## HIGHLIGHTS

- The presence of MPs shortened the granulation time.
- MPs acted as the inducible nucleus to accelerate sludge granulation.
- MPs addition enhanced non-Newtonian flow characteristics of sludge.
- MPs addition improved the removal efficiency of pollutant.
- The formed AGS by applying MPs had a four-layer structure.

## GRAPHICAL ABSTRACT



## ARTICLE INFO

### Keywords:

Mycelial pellets  
Aerobic granular sludge  
Membrane bioreactor

## ABSTRACT

This study provides a sustainable manner for direct cultivation of aerobic granular sludge (AGS) by addition of mycelial pellets (MPs) into continuous-flow aerobic MBR. The results showed that the granulation time in MPs-MBR was shortened by at least 65 days, accounting for enhanced mean size of granules (0.68–0.76 mm), increased mixed liquor suspended solids (MLSS) concentration (12.8 g/L) and improved settling ability (78.1 mL/g), in comparison with that of 0.23–0.28 mm, 9.8 g/L and 102.1 mL/g in control MBR. MPs-MBR demonstrated significant advantages in terms of COD reduction (97.0–99.1%),  $\text{NH}_4^+\text{-N}$  reduction (100%) and TN reduction (32.27–42.33%). MPs, extracellular polymeric substances (EPS) and filamentous bacteria acted as inducible nucleus, crosslinking matter and supporting skeleton, respectively, in favor of promoting the formation and stabilization of AGS with a four-layered structure. The relevant mechanism was underlined by rheological analysis, indicating that MPs addition enhanced non-Newtonian flow characteristics and network structure of sludge.

## 1. Introduction

Since granulation of aerobic activated sludge was first cultivated in sequencing batch reactor (SBR) since 1990 (Morgenroth et al., 1997), a great advance has been made on granular activated sludge (AGS) for both domestic and industrial wastewater treatment (Adav et al., 2008).

It has been well recognized that, compared with activated sludge, the AGS has several unique advantages such as dense structure, high biomass, excellent settleability, biodegradation ability, less excessive sludge production, minimal concern on bulking sludge (Purba et al., 2020), as well as good performance of organic, nitrogen and phosphorous removal (Sarma et al., 2017). This makes AGS the most promising

\* Corresponding author.

E-mail address: [guohaijuan@hebeu.edu.cn](mailto:guohaijuan@hebeu.edu.cn) (H. Guo).

<https://doi.org/10.1016/j.biortech.2021.126233>

Received 20 September 2021; Received in revised form 19 October 2021; Accepted 23 October 2021

Available online 28 October 2021

0960-8524/© 2021 Elsevier Ltd. All rights reserved.

bio-technology for the next-generation biological wastewater treatment (Guo et al., 2020). Combining AGS with membrane bioreactor (MBR), i. e. AG-MBR system, is much favored by synergistic virtue of improved quality and stability of effluents, alleviation of membrane fouling (Sajjad et al., 2016), and mitigation of sludge bulking and collapse in AGS systems during long-term operation (Show et al., 2012). However, most of inoculated sludge in AG-MBR system needs to be pre-cultured with AGS collected from sequencing batch reactors (SBR) (Wang et al., 2013) or anaerobic granular sludge from up-flow anaerobic sludge bed (UASB) reactors (Lim and Kim, 2014). This not only increases the cost and complexity of operation and maintenance, but also presents challenge to stabilize the seed AGS, especially in continuous-flow aerobic MBRs (Corsino et al., 2016). In the perspective of practical application, it is more favorable to realize in situ cultivation of AGS in MBR under continuous-flow aerobic conditions.

To this end, it is common practice to directly cultivate AGS in the MBR with internal hydraulic circulation (Chen et al., 2017). In this process, the granules formation in the MBRs was initiated by winding growth of filamentous bacteria (Dai et al., 2020), followed by subsequent attachment of various microbial cells onto filamentous bacteria to form long strip-like sludge that was crimped to gradually form small-size granular sludge under the action of hydraulic shear force (Wu et al., 2018). Nevertheless, the start-up time required for self-cultivated AGS in MBRs with internal circulation was generally longer than 70 days (Chen et al., 2017). Only a recent study reported the use of intertidal wetland sediment (IWS) as inoculant to accelerate AGS formation in MBR, but wide application is hampered due to the lack of eligible IWS and culturing AGS under high salinity condition (Song et al., 2020). Therefore, effective manners are expected for direct and rapid cultivation of AGS in continuous-flow aerobic MBR system.

Mycelial pellets (MPs) are compact and densely packed form of the filamentous region of fungal hyphae with high hydrophobicity due to the involvement of abundant hydrophobins, which facilitates attachment of microbes onto the filaments of MPs (Zhang et al., 2011). They are advantageous in degrading organic pollutants on account of the production of enzymes, and they possess good adsorption ability as a result of porous structure and large specific area (Espinosa-Ortiz et al., 2016). As biomass material, the MPs have been demonstrated capable of accelerating granulation of aerobic sludge and enhancing long-term stability of AGS in SBR (Geng et al., 2021). Previous study also found the promotion of microbial aggregation by MPs to be the dominant mechanism for mitigating membrane fouling in MBR system (Xiao et al., 2021). It is known that the microbial aggregation was the first step of sludge granulation, thereby the time required for granulation could be shortened by increasing the aggregation rate (Geng et al., 2020). Inspired by these findings, it is feasible to use MPs to accelerate sludge granulation in continuous-flow aerobic MBR. However, comprehensive understanding on the role of MPs in MBR system prone to the overgrowth of filamentous bacteria is limited. Therefore, the process and mechanism of aerobic granulation induced by MPs under such conditions need to be further studied.

On the other hand, rheological behavior of suspended sludge liquid was shown to be of importance in the formation of granular sludge (Wang et al., 2016), due to non-Newtonian and viscoelastic properties of suspended sludge in nature (Laera et al., 2007). The rheological analysis could characterize internal microstructure and physicochemical interaction between extracellular polymeric substances (Eshtiaghi et al., 2013). The inter-linkage between rheological dynamics properties and granule-granule interactions was explored in granular sludge system (Ma et al., 2014). When oscillatory sweeps were conducted, the peculiar viscoelastic response of granular sludge could be indicator to distinguish granular sludge from other sludge systems (Ma et al., 2014). Since the MPs can secrete EPS with similar properties as cross-linking substances in adhesive ability (Wargenau and Kwade, 2010), the addition of MPs will inevitably change the rheological behavior of sludge liquid. This necessitates the rheological analysis to provide in-depth mechanistic

insight into granulation process in MBR in the presence of MPs by creating the relationship between rheological parameters and sludge properties.

The object of this study was to investigate the enhanced in situ granulation of aerobic sludge by MPs in continuous-flow aerobic MBR system. Two lab-scale MBRs were operated for 170 days in parallel under the identical conditions. The granular sludge particle size distribution, EPS, morphological characteristics of sludge were analyzed to illustrate the granulation of sludge in MBR system. The role of MPs in the formation of granular sludge was elucidated in the context of rheological characterization and viscoelasticity measurement, which provided the data basis for further application.

## 2. Materials and methods

### 2.1. Experimental set-up and operating procedures

Two rectangular-shaped MBRs (i. e. MBR and MPs-MBR in the absence and presence of MPs) with an effective volume of 15 L were operated for 170 days under continuous condition. MPs with diameter of 0.8–1.2 mm were added into the MPs-MBR with the pre-determined 20% ratio ( $W_{\text{MPs}}/W_{\text{sludge}}$ ), and the MPs was prepared according to the procedures described in the previous studies (Xiao et al., 2021). The spores suspension of *Aspergillus Niger 557* was inoculated into 150 mL of liquid medium composed of 20.0 g/L glucose, 1 g/L  $\text{NH}_4\text{Cl}$ , 1 g/L  $\text{KH}_2\text{PO}_4$ , and 0.5 g/L  $\text{MgSO}_4 \cdot 7\text{H}_2\text{O}$  in a 250-mL flask. The MPs were obtained after 3-days culture at a rotation speed of 160 rpm at 30 °C.

The two MBRs were individually equipped with polyvinylidene fluoride (PVDF) hollow membrane modules (Yihong Membrane Technology Co., LTD, Jiangsu) with total membrane area of 0.43 m<sup>2</sup> and membrane pore size of 0.3 μm. Unless stated otherwise membrane permeate flux was maintained to be 3.0 LMH throughout the experiments. The membrane module was taken out for cleaning at critical TMP of about 30 kPa. The two microporous tube aerators were installed at the bottom of each MBR to supply dissolved oxygen at a flow rate of 6 L/min. Both MBRs were operated at a solid retention time (SRT) of 30 d and hydraulic retention time (HRT) of 12 h during the 170-day operation. The sludge for inoculating the MBRs was collected from the aeration tank of Wenchang municipal wastewater treatment plant in Harbin City of China. The concentration of mixed liquor suspended solids (MLSS) for inoculation of each MBR was controlled 6.0 g/L. The two reactors were fed with synthetic wastewater with composition (see Supporting Information), and the influent quality of synthetic wastewater contained organic matter (490–530 mg/L COD), nitrogen (46–54 mg/L  $\text{NH}_4^+\text{-N}$ , 2.0–2.5 mg/L  $\text{NO}_3^-\text{-N}$ , 67–73 mg/L TN) and phosphate (4.2–5.0 mg/L TP).

### 2.2. Morphological characterization

The granule size distribution (Mastersizer 2000, Malvern Instruments Ltd., UK) in two MBRs were measured to verify the formation of sludge granules. A digital camera (Canon, Japan) and an optical microscope with a digital camera (CX33, Olympus Corporation, Japan) were used to observe overall size and morphology of sludge granules. An optical coherence tomography (OCT, BaySpec, USA) and a super depth of field digital microscope (DCM8, Leica, Germany) was applied to visualize the three-dimensional structure and densification of granules. The micro-structure of sludge granule was also characterized by scanning electron microscopy (Sigma 500, ZEISS Inc., Germany) using the modified pretreatment method (Wang et al., 2020).

### 2.3. Rheological measurement

The rheological behavior of mixed sludge was measured using a rotational rheometer (Anton Paar MCR302, Austria). The temperature

was held at  $25 \pm 0.1^\circ\text{C}$  using a Peltier controller. The constant angular frequency (5 rad/s) was maintained and the strain was varied from 0.1 to 100% to investigate the structural property of sludge and gain the linear viscoelastic region. The shear rate was increased linearly from 0.1 to  $800\text{ s}^{-1}$  and remained at  $800\text{ s}^{-1}$  for 30 s. And then the shear rate was decreased linearly from  $800$  to  $0.1\text{ s}^{-1}$ . AGS is a shear-thinning fluid with yield pseudoplasticity, similar to Herschel-Bulkley fluid (Ma et al., 2014), and its rheological property belongs to non-Newtonian behavior (Amiraftebi and Khiadani, 2019). The Herschel-Bulkley model (Eq. (1)) was applied to fit the rheological data (Yousefi et al., 2020).

$$\tau = \tau_y + k\dot{\gamma}^n \quad (1)$$

where  $\tau$  is the shear stress (Pa),  $k$  the consistency index ( $\text{Pa}\cdot\text{s}^n$ ),  $\dot{\gamma}$  the shear rate ( $\text{s}^{-1}$ ) and  $n$  the flow behavior index (dimensionless) (Liang et al., 2020).  $\tau_y$  is the yield stress reflecting the structural strength of sludge, which indicates the shear stress to be overcome for the sludge flow (Laera et al., 2007).

The apparent viscosity  $\eta_a$  ( $\text{Pa}\cdot\text{s}$ ) represents the ratio between shear stress and shear rate, which is listed below (Eq. (2)).

$$\eta_a = \frac{\tau}{dv/dy} \quad (2)$$

The apparent viscosity can be used to describe the variations in viscosity of sludge samples when sheared.

## 2.4. Analytics

The determinations of chemical oxygen demand (COD), (ammonium nitrogen)  $\text{NH}_4^+\text{-N}$ , (nitrite nitrogen)  $\text{NO}_2^-\text{-N}$ , (nitrate nitrogen)  $\text{NO}_3^-\text{-N}$ , (total nitrogen) TN, MLSS and  $\text{SVI}_{30}$  were analyzed according to standard methods (APHA, 2005). EPS were extracted from the sludge suspension samples in MPs-MBR and MBR according to the modified thermal extraction method (Zhang and Jiang, 2019). Polysaccharides and proteins analysis were determined by modified phenol-sulfuric acid (Dubios et al., 1956) and Lowry methods (Lowry et al., 1951), respectively.

## 3. Results and discussion

### 3.1. Granulation of aerobic sludge

The significant differences between MPs-MBR and MBR were observed during the process of sludge granulation. As shown in Fig. 1, there was an observation of similar mean sizes of seed sludge measured in MPs-MBR (0.087 mm) and MBR (0.085 mm). The mean size of granules increased from 0.22 mm (day 40) to 0.51 mm (day 80), and then up to 0.68 mm (day 110) in MPs-MBR. From day 110, the mean size of granules was sustained at the diameter of 0.68–0.76 mm, indicating relatively stable distribution of particle size in MPs-MBR within the following days (Fig. 1a). Fig. 1b illustrates the decline in fraction of floc sludge from day 50 to day 120 in MPs-MBR, indicating sludge granulation in progress. In comparison, the mean size of sludge in MBR was

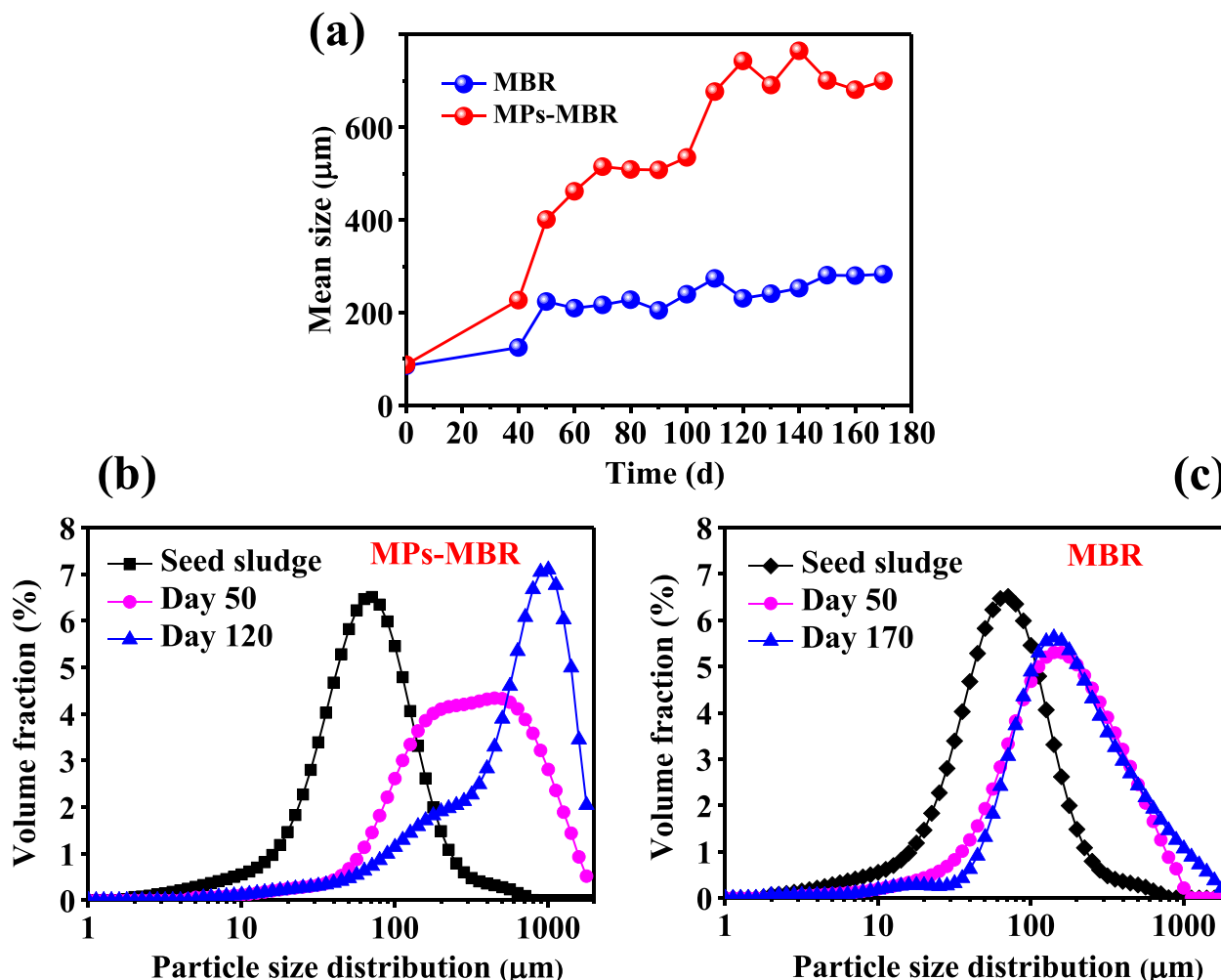


Fig. 1. Mean size of granules (a) and particle size distribution in MPs-MBR (b) and MBR (c).

observed to change insignificantly from 0.22 mm (day 50) to 0.28 mm (day 170), implying the predominance of floc sludge (<0.2 mm) and slow sludge granulation in naturally cultivated conditions without MPs (Fig. 1a and c).

The setting property of sludge was evaluated in terms of  $SVI_{30}$  as an indicator (Iorhemen et al., 2018) under the inoculated sludge of 6.0 g/L in both reactors. As a result of addition of MPs (20%,  $W_{MPs}/W_{sludge}$ ), the initial concentration of MLSS in MPs-MBR (7.2 g/L) was higher than that in MBR (6.0 g/L). Fig. 2a reveals the four typical phases of granule development identified in MPs-MBR, i. e. aggregation (day 1–40), germination (day 40–80), formation (day 80–120) and stabilization (day 120–170).

In the phase of aggregation (day 1–40), the MLSS concentration in MPs-MBR and MBR underwent decrease to 5.2 g/L (day 10) and 4.6 g/L (day 10) followed by increase to 7.2 g/L (day 40) and 6.7 g/L (day 40). The  $SVI_{30}$  value measured for MPs-MBR and MBR was increased greatly from 58.4 mL/g and 55.7 mL/g to 172.9 mL/g and 180.6 mL/g on day 1–10, respectively. During days 10–40, a remarkable decrease in  $SVI_{30}$  in the two MBRs was noticed with the values in MPs-MBR being always lower than that in MBR. In the first 10 days, the poor settleability was mainly caused by over-growth of filamentous bacteria in the two MBRs verified by the results of sludge images shown in Supporting Information, due to higher growth superiority and greater tolerance of filamentous bacteria than that of floc bacteria under substrate-limited condition (Martins et al., 2004). In general, overgrowth of filamentous bacteria in conventional activated sludge system (e. g. SBR) might be

subject to biomass loss and eventual failure of bioreactor resulting from the poor sludge settleability under high selection pressure (Liu and Liu, 2006). On the contrary, negligible selection pressure in MBR was more beneficial for the biomass retention, with positive effects on the formation of granular sludge (Chen et al., 2017). The filamentous bacteria with long and dense filament could play a role of skeleton necessary for attachment of other bacteria and floc sludge to form microbial aggregation (Dai et al., 2020). However, the granulation proceeded by filamentous bacteria occurred at a slow rate because of dependence on the adhesion and entanglement of filamentous bacteria and microbial cells under specific hydraulic shear force (Song et al., 2020). This would result in much longer time needed for the formation of initial agglomerates in MBR (80 days) and confirmed by the optical microscope images in Supporting Information, which appeared to be in line with previous studies (Chen et al., 2017). On the contrary, although the inadaptability of MPs to micro-environment, the phagocytosis by metazoans due to high protein content of MPs and the detachment caused by hydraulic shear force may lead to their decomposition, mycelial debris remained in MPs-MBR still acts as natural nucleus, providing pores and channels for attachment and reproduction of microorganisms including both floc and filamentous bacteria (FOMINA and GADD, 2002). The introduction of MPs could greatly provoke agglomeration of floc sludge and hence improved sludge settleability.

In the phase of germination (day 40–80), a significant increase in the MLSS concentration in MPs-MBR was observed from 7.2 g/L to 9.6 g/L, higher than that in MBR (from 6.7 g/L to 7.7 g/L). Correspondingly, the

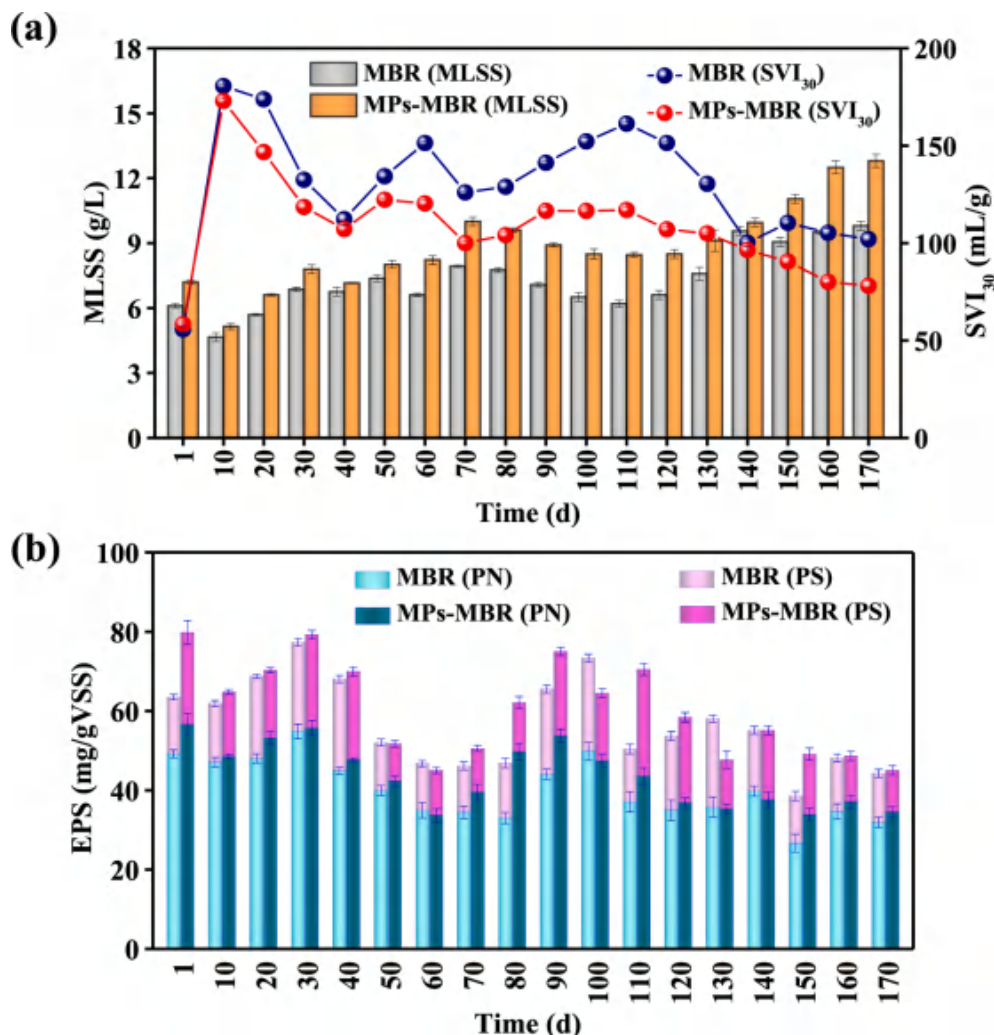


Fig. 2. Variation of MLSS concentration and sludge settling property (a); variation of EPS components (b).



SVI<sub>30</sub> value in MPs-MBR was found to fluctuate between 100.1 mL/g and 122.2 mL/g, while that in MBR between 112.3 mL/g and 151.5 mL/g. During this process, the microbial aggregates in MPs-MBR could be observed to proliferate and form small granules visible to the naked eye (Supporting Information). However, the sludge system in MBR was still dominated by long strip-like filamentous bacteria due to the slower aggregation rate of microorganisms in the absence of MPs, resulting in the poor sludge settleability.

In the phase of formation (day 80–120), the MLSS concentration in MPs-MBR and MBR was found to maintain at approximately 8.5–9.6 g/L and 6.2–7.7 g/L, respectively. The SVI<sub>30</sub> value in MPs-MBR was stabilized at approximately 110 ± 6.5 mL/g, while that in MBR underwent increase from 128.9 mL/g (day 80) to 161.3 mL/g (day 110) followed by decrease to 151.4 mL/g (day 120). During this phase, the long strip-like filamentous bacteria in MBR was gradually curled to form the tiny granule, while a large amount of mature granular sludges could be observed in MPs-MBR with the representative images given in Supporting Information. These results were in good coincidence with the rapid increase in mean size of granules observed in MPs-MBR (Fig. 1).

For the phase of stabilization (day 120–170), clearly visible is a significant increase in MLSS concentration from 8.5 g/L to 12.8 g/L and a considerable decline in SVI<sub>30</sub> value from 107.1 mL/g to 78.1 mL/g in MPs-MBR. Notably, SVI<sub>30</sub> value below 80 mL/g can be a clear indicator for sludge granulation (Toh et al., 2003). As a comparison, the MLSS concentration in MBR was found to increase from 6.6 g/L to 9.8 g/L and the SVI<sub>30</sub> value in MBR underwent decline from 151.4 mL/g to 102.1 mL/g. Compared with MBR, the enhanced biomass concentration, improved settling ability, increased mean size of granules and reduced granulation time in MPs-MBR implied the essential role played by MPs in accelerating sludge granulation. Above results can be achieved by only 20% ( $W_{MPs}/W_{sludge}$ ) MPs addition, which indicates that the MPs possesses practical application potential for AGS cultivation in terms of operation viability and economic applicability in MBR system.

EPS is well known to promote microbial aggregation and sludge granulation due to the property of highly hydrated gel matrix (Corsino et al., 2017). The contents of protein (PN) and polysaccharide (PS) were determined to further illustrate the effect of MPs on EPS secretion during sludge granulation. As shown in Fig. 2b, in the initial period of operation (day 1–40), the higher values of PN and PS in MPs-MBR were always observed in comparison with that in MBR. Especially on day 1, the contents of PN (56.65 mg/g VSS) and PS (23.17 mg/g VSS) in MPs-MBR were much higher than that of 49.21 mg/g VSS and 14.27 mg/g VSS in MBR. This clearly indicated that the addition of MPs remarkably enhanced the PN and PS contents in MPs-MBR, which created favorable conditions for the adhesion and agglomeration between floc sludge and microorganisms via decreasing the repulsive force between microbial cells (Corsino et al., 2017). During days 40–70, 29.3% and 50.6% reduction of PN and PS were detected in MPs-MBR, the values being higher than those in MBR (23.45% and 49.0%). This was likely due to the utilization of part of free EPS in mixed liquor for the adhesion and aggregation of microorganisms to form initial tiny granules in MPs-MBR. As the granulation proceeded to day 80–120, the PN content underwent increase first followed by reaching the maximum of 53.77 mg/g VSS and further decrease to 36.9 mg/g VSS in MPs-MBR, the values being also larger than that in MBR (from 49.85 mg/g VSS to 33.01 mg/g VSS). Higher PS content was also observed in MPs-MBR (17.10–26.91 mg/g VSS) compared with that in MBR (13.31–23.48 mg/g VSS). It can be considered that higher amount of PN and PS should be responsible for the increase in particle size and the acceleration of sludge granulation in MPs-MBR (Geng et al., 2021). In this phase, the improvement of EPS content in MPs-MBR should be mainly caused by the increase in biomass concentration. During the prolonged phase of operation (day 120–170), the PN and PS contents in MPs-MBR were stabilized over the range of 33.88–37.56 mg/g VSS and 10.50–17.58 mg/g VSS, respectively, with observation of a considerable fluctuation in MBR (26.67–39.76 mg/g VSS in PN, 11.9–22.29 mg/g VSS in PS). This appeared to be in line with

previous study where EPS was secreted more in the stage of granule formation and relatively stable in the stage of stabilization (Dai et al., 2020), suggesting that microorganisms would adjust the EPS production with the changes of the internal environment (Liu et al., 2004).

### 3.2. Overall treatment performances

The performances of pollutant removal in two MBRs were monitored under continuous-flow mode within an operational time span of 170 days. As shown in Fig. 3a, the filamentous bulking and biomass reduction provided the explanation to a slight decline in COD removal efficiency for MPs-MBR and MBR on day 5–20. From day 20 on, the effluent COD concentration in MPs-MBR and MBR were found to stabilize in the range of 7.98–12.53 mg/L and 11.56–16.41 mg/L, respectively, accounting for the COD removal efficiency of 97.0–99.1% for MPs-MBR and 96.4–98.6% for MBR. Fig. 3b, c and d showed the removal efficiencies of NH<sub>4</sub><sup>+</sup>-N, NO<sub>2</sub><sup>-</sup>-N, NO<sub>3</sub><sup>-</sup>-N and TN during the whole period of operation. The NH<sub>4</sub><sup>+</sup>-N was removed with the overall efficiency approaching 100% and negligible NO<sub>2</sub><sup>-</sup>-N accumulation in two MBRs (<0.5 mg/L), indicating the excellent nitrification capability in two systems. During the operation of days 1–50, NO<sub>3</sub><sup>-</sup>-N accumulation should be responsible for low TN removal efficiency, due to weak denitrifying performance relevant to inhibition of high-concentration DO (>4 mg/L) in two MBRs (Nancharaiah et al., 2016). With the extension of operating time on day 50, there was an observation of decrease in NO<sub>3</sub><sup>-</sup>-N accumulation and increase in TN removal in MPs-MBR. Notably, during day 110–170, TN removal efficiency in MPs-MBR reached a stable and significant level of 32.27–42.33%, which was much higher than that in MBR (14.14–20.42%). The most likely reason for this was the formation of large amounts of AGS with inner channels and tight shell, creating micro-porous anoxic zones for denitrification (Nancharaiah and Kiran Kumar Reddy, 2018). Notably, functional bacteria involved in nitrogen removal, such as *Nitrospira*, were enriched in MPs-MBR on day 120 (Supporting Information), which greatly enhanced the efficiency of wastewater treatment (Wen et al., 2020). Besides that, granulation of aerobic sludge in MBR has been reported to be efficient in organic pollutants removal through biodegradation, bioaccumulation and biosorption (Purba et al., 2020; Sarma et al., 2017). These results indicated that MPs to be a promising bio-carrier for pollutants removal in favor of enrichment of functional microorganisms for accelerating aerobic sludge granulation in MPs-MBR.

### 3.3. Morphological properties of granular sludge

The granular sludge formed in different stages of operation was collected using the screen mesh (aperture of 0.7 mm) to study the effect of MPs on sludge granulation. The brown small-sized granules with relatively loose boundary and compact kernel on day 55, followed by subsequent formation of more regular-shaped granules with white-margin and brown-center on day 85. The white-margin of granules formed was significantly loose with good light transmittance and more compact brown-colored center. With the extension of operating time, various microorganisms containing hydrophobic substances began to gradually attach onto the white-colored surface of shell, resulting in the formation of larger-size granule with yellow-margins and brown-center. These granules were squeezed to the sphere or ellipse shape with a thicker center under the hydrodynamic shear. With increased number of microorganisms colonized, the granules with brown-margin and black-center emerged in MPs-MBR on day 110, suggesting significant densification and opaque in granules. During the prolonged operation, one could see the formation of black and dense granule as a result of enhanced microbial attachment potential and ongoing hydraulic shear force. The dominant granular sludge exhibited excellent settling ability in MPs-MBR, which appeared to be consistent with the increase in particle size in MPs-MBR on day 120 and observation in previous studies (Wu et al., 2018). On the contrary, it took much longer time to form the

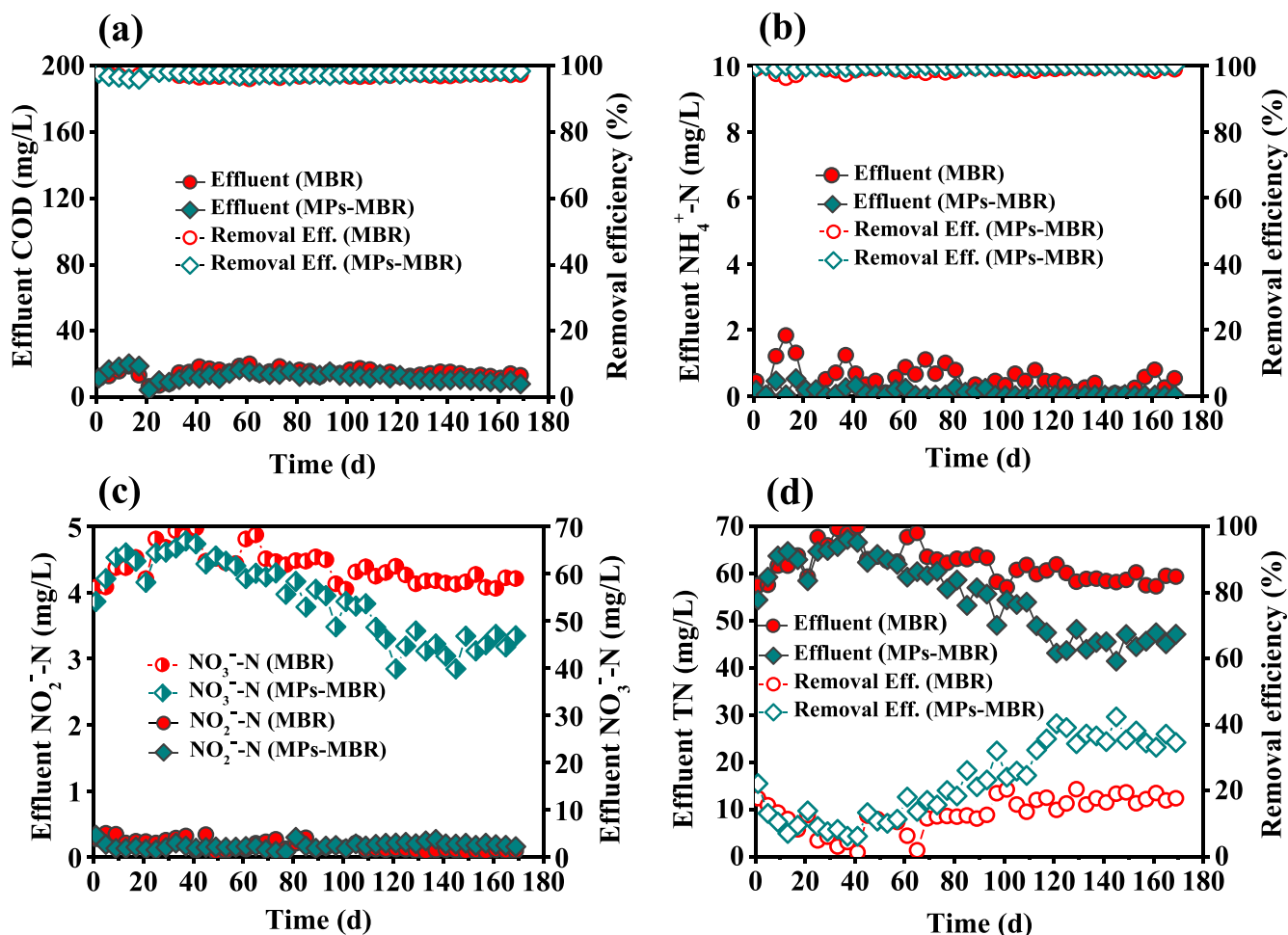


Fig. 3. The effluent concentration and removal efficiency of pollutants during the operation time, (a) COD, (b)  $\text{NH}_4^+\text{-N}$ , (c)  $\text{NO}_2^-\text{-N}$  and  $\text{NO}_3^-\text{-N}$ , (d) TN.

white-margin and brown-center granules with loose outer layer and tiny inner core in the absence of MPs in MBR on day 150. In other words, the granule development in MBR underwent at least 65-day lag behind that in MPs-MBR, but even so the granulation process was still in its infancy in MBR. Therefore, the presence of MPs was the key to accelerating the sludge granulation by promoting the formation of initial core in a much shorter period.

The microscopic structure of granules in MPs-MBR might provide qualitative explanation to the reason for the formation of granules with different colors. Many bacilli cells, floc sludge and few filamentous microorganisms were observed on the surface of brown-colored and small-sized granules (Chen et al., 2017). These granules that were densely covered and twined by the growing filamentous bacteria formed white-colored shells. And then, the adhesion of rod-shaped and globular bacteria on the outer layer was dominated by filamentous bacteria (Dai et al., 2020), resulting in the formation of yellow-margin and brown-centered granules. In the next stage, the tight attachment of rod-shaped and globular bacteria should be responsible for the formation of brown-margin and black-centered granules, creating the aerobic/anoxic micro-environments requisite for biochemical reactions relevant to organic removal and nitrogen (Geng et al., 2021). With the extension of running time, some colloidal substances were also found to firmly wrap and cover the surface of microorganisms, forming the shell structure that was protective on the surface of black granule. In addition, the sectional SEM images identified the layered structure of mature granule to have a four-layer structure with the pores and channels provided by the MPs in the inner nuclear layer. A mass-transfer layer with a number of large-sized pores by filamentous bacteria provided the supporting

skeleton and channels to facilitate the diffusion of nutrients and oxygen (Geng et al., 2021). The attachment of colonizing microorganisms and their secretions between the pores and channels in the third layer, *i. e.* the tight adhesion layer. The outmost hydrophobic layer was composed of microbial cells tightly covered with hydrophobic substances involved in EPS. The representative photographs of granules were shown in Supporting Information.

### 3.4. Rheological properties of sludge system

Rheological behavior of the sludge was examined to reveal the effect of MPs addition on sludge granulation. Table 1 summarized the rheological parameters for the sludge samples on the basis of Herschel-Bulkley model. Compared with that of MBR in the absence of MPs, the decline in  $n$  value combined with increase in  $\tau_y$  and  $k$  values on day 85, indicating the addition of MPs to enhance non-Newtonian flow characteristics and network structure of sludge (Liang et al., 2020). With the extension of operating time on day 85–125, there was an observation of

Table 1  
Fitting results of the Herschel-Bulkley model and the key parameters at sludge samples of two MBRs.

| Items   | Herschel-Bulkley parameters |            |        | Mean $R^2$ |        |
|---------|-----------------------------|------------|--------|------------|--------|
|         | $\tau_y$ (Pa)               | $k$ (Pa·s) | $n$    |            |        |
| MPs-MBR | Day 85                      | 0.0983     | 0.1443 | 0.5693     | 0.9962 |
|         | Day 125                     | 0.0437     | 0.0106 | 0.8313     | 0.9846 |
| MBR     | Day 85                      | 0.0423     | 0.0373 | 0.6752     | 0.9526 |
|         | Day 125                     | 0.1122     | 0.1473 | 0.5219     | 0.9811 |

decrease in  $\tau_y$  from 0.0983 Pa to 0.0437 Pa and  $k$  from 0.1443 Pa·s to 0.0106 Pa·s, plus increase in  $n$  value from 0.5693 to 0.8313 in MPs-MBR. This suggested that the aerobic sludge granulation in MPs-MBR weakened the non-Newtonian flow characteristics of sludge system (Ma et al., 2014). On the contrary, the MBR free of MPs accounted for increase in  $\tau_y$  value from 0.0423 Pa to 0.1122 Pa and decrease in  $k$  value from 0.0373 Pa·s to 0.1473 Pa·s, and decrease in  $n$  value from 0.6752 to 0.5219. That is, the non-Newtonian flow characteristics of sludge in MBR were strengthened.

Fig. 4a and b illustrated the decline in apparent viscosity with respect to shear rate for all the sludge samples. Fig. 4c and d showed the steady shear stress versus shear rate (from 0 to 800  $s^{-1}$  and back to 0 again) in the mixed sludge samples in two MBRs. In the phase of granules formation (day 85), the sludge in MPs-MBR exhibited higher viscosity and shear stress due to higher MLSS concentration and EPS content compared with that in MBR (Fig. 4a and c). According to the prior studies, the colloidal or soluble substances (Li et al., 2020), biomass concentration (Laera et al., 2007) and shear rate (Hasar et al., 2004) constituted the key factors that affected viscosity and rheological properties of activated sludge. High viscosity could be of extreme importance for interaction between floc and floc/granule in the sludge samples of MPs-MBR, which was conducive to microbial agglomeration. However, with the completion of granulation (day 125), lower viscosity and shear stress were observed in MPs-MBR compared with that in MBR

(Fig. 4b and d). This might be explained by the stability of granular morphology and reduction of EPS content and flocs sludge in mixed liquor in MPs-MBR (Farno et al., 2016).

Fig. 5 illustrated the storage modulus ( $G'$ ) and loss modulus ( $G''$ ) as a function of strain. During strain sweep, the strain region where the  $G'$  is kept constant with strain growth is defined as the linear viscoelastic region (Yuan et al., 2014), whilst the fixed  $G'$  represents the gel strength in the original structure (Li et al., 2020).  $G' > G''$  indicates a decisive role played by gel structure in dominating external forces before reaching the cross-over point (Amiraftebi and Khiadani, 2019). Such point is the intersection where  $G'$  and  $G''$  represent critical transition (Baudez et al., 2013). As shown in Fig. 5a,  $G'$  was greater than  $G''$ , within the linear viscoelastic region in both MBRs, indicating the existence of the larger amounts of gel-like substances that predominated in the sludge systems. The  $G'$  values for sludge sample in MPs-MBR within linear viscoelastic region were decreased from 4.24 Pa to 1.46 Pa, the values being higher than that in MBR (from 0.262 Pa to 0.212 Pa), suggesting the larger gel network strength dominated by EPS in sludge system to promote the AGS formation and enhance the AGS stability (Li et al., 2020). Compared with MBR free of MPs, the significantly higher  $G''$  value in MPs-MBR reflected higher viscosity of sludge liquor (Li et al., 2020), resulting in stronger interaction between flocs and granules. This might provide the most likely rheological explanation to ongoing formation of granules in MPs-MBR on day 80–120. As shown in Fig. 5b, the  $G'$  was always lower

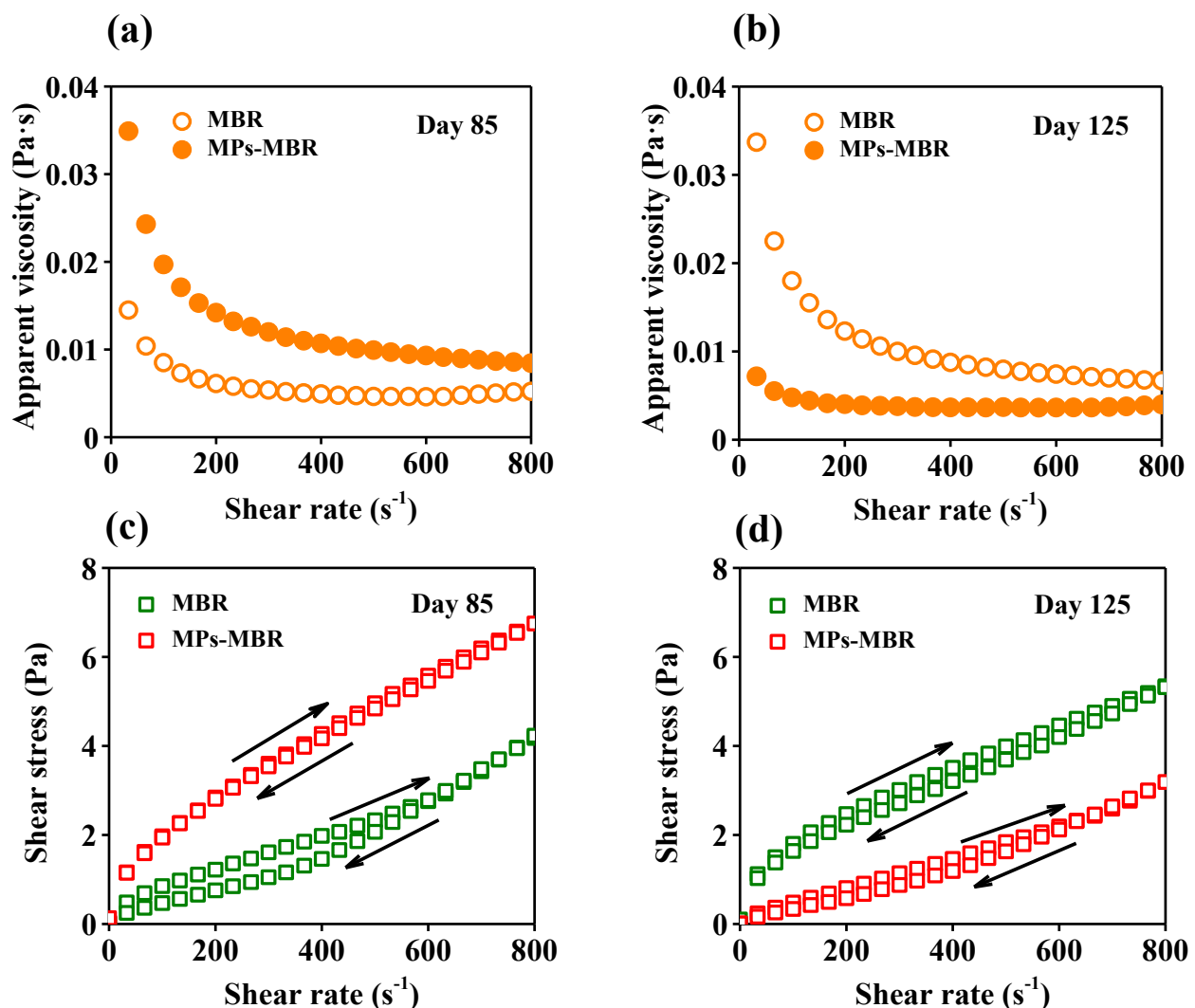


Fig. 4. The apparent viscosity with shear rate (a, b) and shear stress with shear rate (c, d) for the sludge samples on day 85 and day 125.

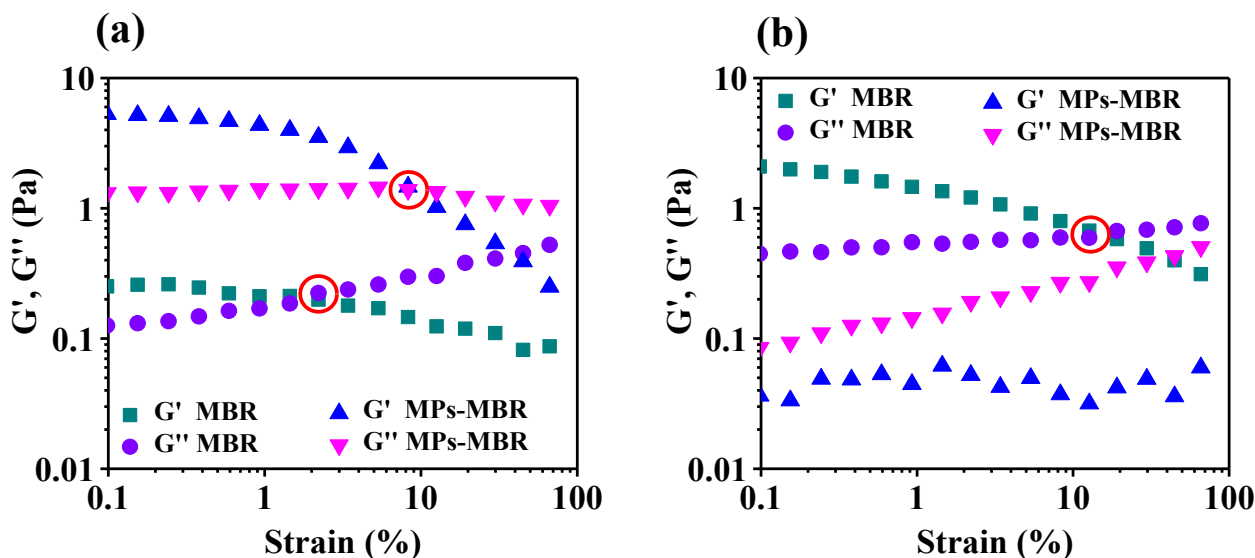


Fig. 5. Storage modulus ( $G'$ ) and loss modulus ( $G''$ ) as a function of strain for the sludge samples (a) on day 85 and (b) day 125.

than  $G''$  in MPs-MBR, indicating that sludge system tended to be a shear-thinning fluid with the extension of operating time (Wang et al., 2016). Large amounts of gel-EPSs were used for the formation of granules to decline in free gel-EPSs and viscosity in the mixed liquor. This was in line with previous study where the viscoelasticity of liquid-like aerobic granules was consistent with that of water, suggesting very close activation energy and molecular movements being involved in the liquid-like regimes of both granules and flocs (Ma et al., 2014). On the contrary, the intersection of  $G'$  and  $G''$  in MBR was observed at a higher certain strain (12.7%), being similar as that in MPs-MBR on day 85. Besides that, an increase in gel-structure of MBR should be responsible for the large linear viscoelastic region on day 125. The rheological evidence supported the role of MPs in accelerating the granulation of sludge in MBR.

### 3.5. Mechanism of sludge granulation in the presence of MPs in MBR

To further gain mechanistic insight into the effect of MPs on sludge granulation and rheological behavior, the particle volume fraction (PVF) was examined in the mixed sludge. As shown in Table 2, the PVF values for MPs-MBR on day 85 followed the order of  $D_{0.2-0.5\text{mm}}$  (granules with a diameter of 0.2–0.5 mm, 37.14%) >  $D_{0.5-1\text{mm}}$  (granules with a diameter of 0.5–1 mm, 27.19%) >  $D_{<0.2\text{mm}}$  (granules with a diameter of smaller than 0.2 mm, 23.24%) >  $D_{>1\text{mm}}$  (granules with a diameter of larger than 1 mm, 12.43%). As granulation proceeded to day 125, the highest PVF of  $D_{0.5-1\text{mm}}$  was observed (33.63%), followed by  $D_{>1\text{mm}}$  (30.37%),  $D_{0.2-0.5\text{mm}}$  (18.93%) and  $D_{<0.2\text{mm}}$  (17.07%) in order. By contrast, the sludge system in MBR was always dominated by  $D_{<0.2\text{mm}}$  granules, followed by the sequence of  $D_{0.2-0.5\text{mm}}$ ,  $D_{0.5-1\text{mm}}$  and  $D_{>1\text{mm}}$ . The improved PN and PS

Table 2

The particle volume fraction (PVF) of mixed sludge in two MBRs on day 85 and day 125.

| Items   |         | Particle volume fraction (%) |                        |                      |                   |
|---------|---------|------------------------------|------------------------|----------------------|-------------------|
|         |         | $D_{<0.2\text{mm}}$          | $D_{0.2-0.5\text{mm}}$ | $D_{0.5-1\text{mm}}$ | $D_{>1\text{mm}}$ |
| MPs-MBR | Day 85  | 23.24 ± 0.24                 | 37.14 ± 0.11           | 27.19 ± 0.12         | 12.43 ± 0.32      |
|         | Day 125 | 17.07 ± 0.11                 | 18.93 ± 0.15           | 33.63 ± 0.22         | 30.37 ± 0.25      |
| MBR     | Day 85  | 55.08 ± 0.31                 | 31.57 ± 0.56           | 11.46 ± 0.41         | 1.89 ± 0.25       |
|         | Day 125 | 54.44 ± 0.44                 | 37.68 ± 0.63           | 6.37 ± 0.58          | 1.51 ± 0.16       |

caused by MPs addition were capable of sustaining the gel structure of EPS in MBR, which constituted an essential factor to promote the flocs aggregation and hence to form the initial core of AGS with a diameter of 0.2–0.5 mm on day 1–80 (Fig. 1 and Supporting Information). Higher amount of free gel-like EPS and granules in MPs-MBR gave rise to a higher resistance to deformation of AGS compared with that in MBR (Wang et al., 2016). This corresponded well to the observation of larger viscosity, yield stress and  $G'$  values of the sludge mixture on day 85 (Fig. 4 and Fig. 5). This should be the most probable reason for the increased collision probability of small granules with flocs and EPS in mixed liquor and the formation of granules with a diameter > 0.5 mm. On day 120–170, clearly visible is a decline in the free gel-like EPS in the mixed liquor, accompanied by the formation of >80% granules (>0.2 mm). The PVF values of  $D_{0.2-0.5\text{mm}}$  granules were decreased significantly with considerable increase in  $D_{>0.5\text{mm}}$  granules, being in line with lower viscosity, yield stress and  $G'$  values in mixed sludge (Ma et al., 2014).

It is worth emphasizing that the conditions offered by MBR are essential to enhanced granulation of sludge. Long HRT of 12 h and continuous-flow mode provided environment suitable for the overgrowth of filamentous bacteria under the limited nutrient substrate, whilst long SRT of 30 d and negligible selection pressure facilitated the maintenance of abundant biomass and high MLSS concentration in MBR. Under such operating conditions, the mechanism of sludge granulation on a qualitative basis was proposed to schematically illustrate the sludge granulation promoted by MPs in aerobic MBR under the continuous-flow mode, which could be described as (a) the presence of MPs, (b) filamentous bacteria, (c) gel-like EPS. In details, the MPs not only promoted the formation of initial core via abundant EPS and adsorption by large surface area (Geng et al., 2021), but also strengthened internal structure via hyphae matrix (FOMINA and GADD, 2002). The entanglement of filamentous bacteria could act as supporting skeleton to compact granule structure and provide sites for attachment of multiple microbial communities (Figuerola et al., 2015). The gel-like EPS, including hydrophobin and polysaccharides, offered cross-linking network, thereby the interaction between microbial cells was enhanced to allow the formation of granular sludge with improved mechanical strength (Ma et al., 2014). In addition, the sustainability and stability of hydraulic shear force caused by continuous uniform aeration within the MBR should be responsible for the compact and regular shape of granular sludge. These comprehensive results could be reflected by the rheological behavior of sludge in the phase of granule formation, in terms of enhanced network strength, increased linear viscoelastic regime, improved interaction between granules and flocs, and less



sensitive for the sludge system to shear stress in rheological test, which led to the rapid formation of the unique granules with a four-layer structure. The sludge granulation was a sustained process due to the above combined effects, which was the reason why the time required for sludge granulation was greatly shortened by 65 days in the presence of MPs compared with that for absence. As the PVF value for  $D_{>0.2}$  mm granules increased to a critical ratio (>80%), the EPS content in the mixed liquor tended to be stable, resulting in the shear thinning of granular sludge and the stability of network structure in MPs-MBR.

The mechanism of aerobic sludge granulation in the presence of MPs in MBR reveals more details about how aerobic granulation occurs and how the process can be accelerated. The results confirm that the addition of MPs can directly and rapidly cultivate AGS with enhanced performance in MBR system and it is desirable to provide fundamental and lab-scale investigations for practical engineering application of AG-MBR technology.

#### 4. Conclusion

This study provided a potential approach for rapid in situ granulation by applying MPs in continuous-flow aerobic MBR. The results indicated that the addition of MPs enhanced aerobic sludge granulation with improved granules size and significant pollutants removal. The formed AGS in MPs-MBR had a four-layer structure, in which MPs acted as the inducible nucleus to accelerate the formation of AGS. The role of MPs in sludge granulation was analyzed by rheology, including enhanced network strength of sludge and increased interaction forces between tiny granules and flocs, which shortened the granulation time by at least 65 days.

#### Declaration of Competing Interest

The authors declare that they have no known competing financial interests or personal relationships that could have appeared to influence the work reported in this paper.

#### Acknowledgements

This work was supported by the National Natural Science Foundation of China (No.51878237 and 52070054). We would also like to acknowledge the assistance of Longjiang Environmental Protection Group Co., Ltd and Heilongjiang Touyan Team.

#### Appendix A. Supplementary data

Supplementary data to this article can be found online at <https://doi.org/10.1016/j.biortech.2021.126233>.

#### References

- Adav, S.S., Lee, D.-J., Show, K.-Y., Tay, J.-H., 2008. Aerobic Granular Sludge: Recent Advances. *Biotechnol. Adv.* 26 (5), 411–423.
- Amirafabi, M., Khadani, M., 2019. Transparent polymers to emulate the rheological properties of primary, activated, and digested sludge. *Chem. Eng. Res. Des.* 146, 404–415.
- APHA, 2005. *Standard Methods for the Examination of Water and Wastewater*. American Public Health Association, Washington, DC, USA.
- Baudez, J.-C., Gupta, R.K., Eshtiaghi, N., Slatter, P., 2013. The viscoelastic behaviour of raw and anaerobic digested sludge: Strong similarities with soft-glassy materials. *Water Res.* 47 (1), 173–180.
- Chen, C., Bin, L., Tang, B., Huang, S., Fu, F., Chen, Q., Wu, L., Wu, C., 2017. Cultivating granular sludge directly in a continuous-flow membrane bioreactor with internal circulation. *Chem. Eng. J.* 309, 108–117.
- Corsino, S.F., Campo, R., Di Bella, G., Torregrossa, M., Viviani, G., 2016. Study of aerobic granular sludge stability in a continuous-flow membrane bioreactor. *Bioresour. Technol.* 200, 1055–1059.
- Corsino, S.F., Capodici, M., Torregrossa, M., Viviani, G., 2017. Physical properties and Extracellular Polymeric Substances pattern of aerobic granular sludge treating hypersaline wastewater. *Bioresour. Technol.* 229, 152–159.
- Dai, C., Bin, L., Tang, B., Li, P., Huang, S., Fu, F., Yin, Q., 2020. Promoting the granulation process of aerobic granular sludge in an integrated moving bed biofilm-

- membrane bioreactor under a continuous-flowing mode. *Sci. Total Environ.* 703, 135482. <https://doi.org/10.1016/j.scitotenv.2019.135482>.
- Dubios, M., Gilles, K.A., Hamihon, J.R., Rebers, P.A., Smith, F., 1956. Phenol sulphuric acid method for total carbohydrate. *Anal. Chem.* 350 (26).
- Eshtiaghi, N., Markis, F., Yap, S.D., Baudez, J.-C., Slatter, P., 2013. Rheological characterisation of municipal sludge: A review. *Water Res.* 47 (15), 5493–5510.
- Espinosa-Ortiz, E.J., Rene, E.R., Pakshirajan, K., van Hullebusch, E.D., Lens, P.N.L., 2016. Fungal pelleted reactors in wastewater treatment: Applications and perspectives. *Chem. Eng. J.* 283, 553–571.
- Farno, E., Baudez, J.C., Parthasarathy, R., Eshtiaghi, N., 2016. Impact of thermal treatment on the rheological properties and composition of waste activated sludge: COD solubilisation as a footprint of rheological changes. *Chem. Eng. J.* 295, 39–48.
- Figuerola, M., Val del Río, A., Campos, J.L., Méndez, R., Mosquera-Corral, A., 2015. Filamentous bacteria existence in aerobic granular reactors. *Bioprocess Biosyst Eng* 38 (5), 841–851.
- Fomina, M., Gadd, G.M., 2002. Influence of clay minerals on the morphology of fungal pellets. *Mycological research* 106 (1), 107–117.
- Geng, M., Ma, F., Guo, H., Su, D., 2020. Enhanced aerobic sludge granulation in a Sequencing Batch Reactor (SBR) by applying mycelial pellets. *J. Clean. Prod.* 274, 123037. <https://doi.org/10.1016/j.jclepro.2020.123037>.
- Geng, M., You, S., Guo, H., Ma, F., Xiao, X., Zhang, J., 2021. Impact of fungal pellets dosage on long-term stability of aerobic granular sludge. *Bioresour. Technol.* 332, 125106. <https://doi.org/10.1016/j.biortech.2021.125106>.
- Guo, T., Ji, Y.u., Zhao, J., Horn, H., Li, J., 2020. Coupling of Fe-C and aerobic granular sludge to treat refractory wastewater from a membrane manufacturer in a pilot-scale system. *Water Res.* 186, 116331. <https://doi.org/10.1016/j.watres.2020.116331>.
- Hasar, H., Kinaci, C., Ünlü, A., Toğrul, H., Ipek, U., 2004. Rheological properties of activated sludge in a sMBR. *Biochem. Eng. J.* 20 (1), 1–6.
- Iorhemen, O.T., Hamza, R.A., Zaghoul, M.S., Tay, J.H., 2018. Simultaneous organics and nutrients removal in side-stream aerobic granular sludge membrane bioreactor (AGMBR). *J. Water Process. Eng.* 21, 127–132.
- Laera, G., Giordano, C., Pollice, A., Saturno, D., Mininni, G., 2007. Membrane bioreactor sludge rheology at different solid retention times. *Water Res.* 41 (18), 4197–4203.
- Li, Z., Lin, L., Liu, X., Wan, C., Lee, D.-J., 2020. Understanding the role of extracellular polymeric substances in the rheological properties of aerobic granular sludge. *Sci. Total Environ.* 705, 135948. <https://doi.org/10.1016/j.scitotenv.2019.135948>.
- Liang, J., Zhang, S., Huang, J., Ye, M., Yang, X., Huang, S., Sun, S., 2020. Mechanism of zero valent iron and anaerobic mesophilic digestion combined with hydrogen peroxide pretreatment to enhance sludge dewaterability: Relationship between soluble EPS and rheological behavior. *Chemosphere* 247, 125859. <https://doi.org/10.1016/j.chemosphere.2020.125859>.
- Lim, S.J., Kim, T.-H., 2014. Applicability and trends of anaerobic granular sludge treatment processes. *Biomass Bioenergy* 60, 189–202.
- Liu, Y.u., Liu, Q.-S., 2006. Causes and control of filamentous growth in aerobic granular sludge sequencing batch reactors. *Biotechnol. Adv.* 24 (1), 115–127.
- Liu, Y.Q., Liu, Y., Tay, J.H., 2004. The effects of extracellular polymeric substances on the formation and stability of biogranules. *Appl. Microbiol. Biotechnol.* 65 (2), 143–148.
- Lowry, OliverH., Rosebrough, NiraJ., Farr, A.L., Randall, RoseJ., 1951. Protein measurement with the Folin phenol reagent. *J. Biol. Chem.* 193 (1), 265–275.
- Ma, Y.-J., Xia, C.-W., Yang, H.-Y., Zeng, R.J., 2014. A rheological approach to analyze aerobic granular sludge. *Water Res.* 50, 171–178.
- Martins, A.M.P., Pagilla, K., Heijnen, J.J., van Loosdrecht, M.C.M., 2004. Filamentous bulking sludge—a critical review. *Water Res.* 38 (4), 793–817.
- Morgenroth, E., Sherden, T., Van Loosdrecht, M.C.M., Heijnen, J.J., Wilderer, P.A., 1997. Aerobic granular sludge in a sequencing batch reactor. *Water Res.* 31 (12), 3191–3194.
- Nancharaiyah, Y.V., Kiran Kumar Reddy, G., 2018. Aerobic granular sludge technology: Mechanisms of granulation and biotechnological applications. *Bioresour. Technol.* 247, 1128–1143.
- Nancharaiyah, Y.V., Venkata Mohan, S., Lens, P.N.L., 2016. Recent advances in nutrient removal and recovery in biological and bioelectrochemical systems. *Bioresour. Technol.* 215, 173–185.
- Purba, Laila Dina Amalia, Ibiyeye, Hamzat Tijani, Yuzir, Ali, Mohamad, Shaza Eva, Iwamoto, Koji, Zamyadi, Arash, Abdullah, Norhayati, 2020. Various applications of aerobic granular sludge: A review. *Environ. Technol. Inno.* 20, 101045. <https://doi.org/10.1016/j.eti.2020.101045>.
- Sajjad, Muhammad, Kim, In S., Kim, Kwang Soo, 2016. Development of a novel process to mitigate membrane fouling in a continuous sludge system by seeding aerobic granules at pilot plant. *J. Membr. Sci.* 497, 90–98.
- Sarma, Saurabh Jyoti, Tay, Joo Hwa, Chu, Angus, 2017. Finding Knowledge Gaps in Aerobic Granulation Technology. *Trends Biotechnol.* 35 (1), 66–78.
- Show, Kuan-Yeow, Lee, Duu-Jong, Tay, Joo-Hwa, 2012. Aerobic Granulation: Advances and Challenges. *Appl. Biochem. Biotechnol.* 167 (6), 1622–1640.
- Song, Weilong, Xu, Dong, Bi, Xuejun, Ng, How Yong, Shi, Xueqing, 2020. Intertidal wetland sediment as a novel inoculation source for developing aerobic granular sludge in membrane bioreactor treating high-salinity antibiotic manufacturing wastewater. *Bioresour. Technol.* 314, 123715. <https://doi.org/10.1016/j.biortech.2020.123715>.
- Toh, S., Tay, J., Moy, B., Ivanov, V., Tay, S., 2003. Size-effect on the physical characteristics of the aerobic granule in a SBR. *Appl. Microbiol. Biotechnol.* 60 (6), 687–695.
- Wang, Bin-Bin, Luo, Qin, Li, Hui-Juan, Yao, Qian, Zhang, Lin, Zou, Jin-Te, He, Feng, 2020. Characterization of aerobic granules formed in an aspartic acid fed sequencing batch reactor under unfavorable hydrodynamic selection conditions. *Chemosphere* 260, 127600. <https://doi.org/10.1016/j.chemosphere.2020.127600>.

- Wang, Hou-Feng, Hu, Hao, Yang, Hai-Yang, Zeng, Raymond J., 2016. Characterization of anaerobic granular sludge using a rheological approach. *Water Res.* 106, 116–125.
- Wang, Yaqin, Zhong, Chen, Huang, Dan, Wang, Yongjian, Zhu, Jianrong, 2013. The membrane fouling characteristics of MBRs with different aerobic granular sludges at high flux. *Bioresour. Technol.* 136, 488–495.
- Wargenau, Andreas, Kwade, Arno, 2010. Determination of Adhesion between Single *Aspergillus niger* Spores in Aqueous Solutions Using an Atomic Force Microscope. *Langmuir* 26 (13), 11071–11076.
- Wen, Jianfeng, LeChevallier, Mark W., Tao, Wendong, 2020. Nitrification kinetics and microbial communities of activated sludge as a full-scale membrane bioreactor plant transitioned to low dissolved oxygen operation. *J. Clean. Prod.* 252, 119872. <https://doi.org/10.1016/j.jclepro.2019.119872>.
- Wu, Luying, Tang, Bing, Bin, Liying, Chen, Guangpeng, Huang, Shaosong, Li, Ping, Fu, Fenglian, 2018. Heterogeneity of the diverse aerobic sludge granules self-cultivated in a membrane bioreactor with enhanced internal circulation. *Bioresour. Technol.* 263, 297–305.
- Xiao, Xiao, You, Shijie, Guo, Haijuan, Ma, Fang, Zhang, Jinna, Zhang, Ruiyao, Bao, Xiaotong, 2021. Mycelial pellets for alleviation of membrane fouling in membrane bioreactor. *J. Membr. Sci.* 635, 119545. <https://doi.org/10.1016/j.memsci.2021.119545>.
- Yousefi, Shiva A., Nasser, Mustafa S., Hussein, Ibelwaleed A., Benamor, Abdelbaki, El-Naas, Muftah H., 2020. Influence of polyelectrolyte structure and type on the degree of flocculation and rheological behavior of industrial MBR sludge. *Sep. Purif. Technol.* 233, 116001. <https://doi.org/10.1016/j.seppur.2019.116001>.
- Yuan, D.Q., Wang, Y.L., Feng, J., 2014. Contribution of stratified extracellular polymeric substances to the gel-like and fractal structures of activated sludge. *Water Res.* 56, 56–65.
- Zhang, Si, Li, Ang, Cui, Di, Yang, Jixian, Ma, Fang, 2011. Performance of enhanced biological SBR process for aniline treatment by mycelial pellet as biomass carrier. *Bioresour. Technol.* 102 (6), 4360–4365.
- Zhang, Wenxiang, Jiang, Feng, 2019. Membrane fouling in aerobic granular sludge (AGS)-membrane bioreactor (MBR): Effect of AGS size. *Water Res.* 157, 445–453.